

## Phase Transitions in Films of Lung Surfactant at the Air-Water Interface

Kaushik Nag,\* Jesus Perez-Gil,# Miguel L. F. Ruano,# Lynn Anne D. Worthman,\* June Stewart,\* Cristina Casals,# and Kevin M. W. Keough\*<sup>§</sup>

\*Department of Biochemistry and <sup>§</sup>Discipline of Paediatrics, Memorial University of Newfoundland, St. John's, Newfoundland, Canada A1B 3X9, and #Departamento de Bioquímica y Biología Molecular I, Universidad Complutense, 28040 Madrid, Spain

**ABSTRACT** Pulmonary surfactant maintains a putative surface-active film at the air-alveolar fluid interface and prevents lung collapse at low volumes. Porcine lung surfactant extracts (LSE) were studied in spread and adsorbed films at  $23 \pm 1^\circ\text{C}$  using epifluorescence microscopy combined with surface balance techniques. By incorporating small amounts of fluorescent probe 1-palmitoyl-2-nitrobenzoxadiazole dodecanoyl phosphatidylcholine (NBD-PC) in LSE films the expanded (fluid) to condensed (gel-like) phase transition was studied under different compression rates and ionic conditions. Films spread from solvent and adsorbed from vesicles both showed condensed (probe-excluding) domains dispersed in a background of expanded (probe-including) phase, and the appearance of the films was similar at similar surface pressure. In quasistatically compressed LSE films the appearance of condensed domains occurred at a surface pressure ( $\pi$ ) of 13 mN/m. Such domains increased in size and amounts as  $\pi$  was increased to 35 mN/m, and their amounts appeared to decrease to 4% upon further compression to 45 mN/m. Above  $\pi$  of 45 mN/m the LSE films had the appearance of filamentous materials of finely divided dark and light regions, and such features persisted up to a  $\pi$  near 68 mN/m. Some of the condensed domains had typical kidney bean shapes, and their distribution was similar to those seen previously in films of dipalmitoylphosphatidylcholine (DPPC), the major component of surfactant. Rapid cyclic compression and expansion of LSE films resulted in features that indicated a possible small (5%) loss of fluid components from such films or an increase in condensation efficiency over 10 cycles. Calcium (5 mM) in the subphase of LSE films altered the domain distribution, decreasing the size and increasing the number and total amount of condensed phase domains. Calcium also caused an increase in the value of  $\pi$  at which the maximum amount of independent condensed phase domains were observed to 45 mN/m. It also induced formation of large amounts of novel, nearly circular domains containing probe above  $\pi$  of 50 mN/m, these domains being different in appearance than any seen at lower pressures with calcium or higher pressures in the absence of calcium. Surfactant protein-A (SP-A) adsorbed from the subphase onto solvent-spread LSE films, and aggregated condensed domains in presence of calcium. This study indicates that spread or adsorbed lung surfactant films can undergo expanded to condensed, and possibly other, phase transitions at the air-water interface as lateral packing density increases. These phase transitions are affected by divalent cations and SP-A in the subphase, and possibly by loss of material from the surface upon cyclic compression and expansion.

### INTRODUCTION

Surface active material from the lungs, or pulmonary surfactant (PS) lines the air-alveolar fluid interface with a putative monomolecular film and prevents alveolar collapse at low volumes. In vitro PS shows two specific surface active properties, rapid adsorption to an air-water interface to form surface active films, and the reduction of the surface tension of that interface to low values on compression of such films. The material consists mainly of dipalmitoylphosphatidylcholine (DPPC), unsaturated phosphatidylcholine (PC), and smaller but significant amounts of phosphatidylglycerol (PG), cholesterol, and proteins (King and Clements, 1972). It is proposed that the surfactant proteins SP-A, SP-B, and SP-C enhance its surface spreading prop-

erties (Goerke and Clements, 1986; Keough, 1992). It is presumed the alveolar film undergoes enrichment with DPPC by either selective adsorption of "pools" of secreted materials from the subphase of the film, or by non-DPPC materials being "squeezed out" of the film during successive cycling of the surfactant at the air-alveolar fluid interface, or a combination of both processes (Goerke and Clements, 1986; Keough, 1992; Pison et al., 1996). Although surface films consisting of more than a monolayer have recently been demonstrated (Schürch and Bachofen, 1995), it is not clear to date what the composition of such films are in vivo or in vitro, and whether all or some of the components of PS are involved in maintenance of such films.

Some studies have indicated that surfactant films in the alveoli are almost solid-like in density and highly enriched in DPPC (Bangham, 1987; Goerke and Clements, 1986). There are reports indicating that lung surfactant films undergo a broad lateral phase transition in vitro, with increased packing at the air-water interface (Dluhy et al., 1989; Gulik et al., 1994; Keough et al., 1985; King and Clements, 1972; Lalchev et al., 1996; Träuble et al., 1974). A broad calorimetrically detectable thermotropic phase transition can occur in suspensions of surfactant of most species (Keough,

Received for publication 20 June 1997 and in final form 15 March 1998.

Address reprint requests to Dr. Kevin Keough, Department of Biochemistry, Memorial University of Newfoundland, St. John's, Newfoundland, Canada A1B 3X9. Tel.: 709-737-2530; Fax: 709-737-2552; E-mail: kkeough@morgan.ucs.mun.ca.

Dr. Nag's current address is Department of Obstetrics and Gynaecology, MRC Group in Fetal and Neonatal Health and Development, University of Western Ontario, London, Ontario, Canada N6A 5A5.

© 1998 by the Biophysical Society

0006-3495/98/06/2983/13 \$2.00

1992). The bilayer phase transition is influenced by the hydration states (Teubner et al., 1983), unsaturated lipid content (Hook et al., 1984), calcium (Mautone et al., 1987) and surfactant protein-A (Ge et al., 1995). Fluorescence microscopy of lipid-protein films has become a valuable tool in studying models of biological membranes (Möhwald, 1990; Stine, 1994) and pulmonary surfactant (Nag et al., 1991, 1994, 1996a, b; Discher et al., 1996). By using this technique the two-dimensional expanded (fluid) to condensed (gel-like) phase transitions in lipid and lipid-protein films at the air-water interface can be observed and characterized. Recently Hall and co-workers, using fluorescence microscopy, detected an expanded-to-condensed phase transition in calf lung surfactant films with increased packing of such films, and suggested that the condensed domains are made of mainly DPPC (Discher et al., 1996). In this study we show that a similar phase transition and other transitions occur in solvent-spread and vesicle-adsorbed films of porcine lung surfactant extracts (LSE) using epifluorescence microscopy. We also show that the phase transitions in LSE films at the air-water interface are affected by film cycling, calcium, and surfactant protein-A (SP-A), and found that some properties correlate with previous studies on models using simpler component films (Nag and Keough, 1993; Nag et al., 1990, 1991, 1994, 1996a, b; Perez-Gil et al., 1992).

## MATERIALS AND METHODS

### Materials

The fluorescent probe 1-palmitoyl-2-[12-[(7-nitro-2-1, benzoxadiazole-4-yl)amino] dodecanoyl] phosphatidylcholine (NBD-PC) was obtained from Avanti Polar Lipids (Alabaster, AL). The probe was checked for purity by silica-gel thin layer chromatography and used as received. The subphase buffer was 0.15 M NaCl, 5 mM CaCl<sub>2</sub> in 5 mM Tris-HCl made with doubly distilled deionized water, with the second distillation being from dilute KMnO<sub>4</sub>.

### Isolation of LSE

Pulmonary surfactant was prepared by bronchioalveolar lavage of porcine lungs with 0.15 M NaCl at 4°C (Keough et al., 1985). The lavage was centrifuged for 10 min at 1000 × g to remove cells and debris, and the supernatant was subsequently centrifuged at 20,000 × g for 1 h to pellet the surfactant. The pelleted material was used to extract the hydrophobic materials of lung surfactant using chloroform/methanol/water combinations by the method of Bligh and Dyer (1959). The extracted material is presumed to contain all the lipids and the hydrophobic proteins (SP-B and SP-C) of porcine pulmonary surfactant, and is referred to as the lung surfactant extract (LSE). The phospholipid content was determined using the phosphorus assay of Bartlett (1959) as modified by Keough and Kariel (1987).

### Labeling of SP-A

SP-A was isolated from porcine bronchioalveolar lavage by sequential butanol and octylglucoside extraction by methods discussed elsewhere (Casals et al., 1993). Fluorescent labeling of SP-A was performed as follows. The pH of the buffer (5 mM Tris, pH 7.4) containing SP-A was adjusted to 8.0 by adding 50 mM Tris at pH 8.3. Then 1 mM Texas-Red

isothiocyanate (TR-ITC, Molecular Probes, Eugene, OR) dissolved in methanol was added to the SP-A solution to a final ratio of SP-A/TR-ITC of 10:1 (wt/wt). This solution was incubated at 24°C for 2 h in the dark, and extensively dialyzed for 3 days in the dark against a 5 mM Tris-HCl buffer (pH 7.4) using a 5–24/32 dialysis membrane (Medical International, London, UK). The Texas-Red-labeled SP-A (TR-SP-A) had a monomer molecular weight of ~37 as seen by sodium dodecyl sulfate polyacrylamide gel electrophoresis (SDS-PAGE) and matrix-assisted laser desorption/ionization (MALDI) mass spectrometry performed by methods discussed elsewhere (Nag et al., 1996a; Hillenkamp et al., 1991). The MALDI spectra also indicated that TR-SP-A was mainly in the glycosylated form and was labeled with ~1 mol of Texas-Red per monomer. The details about labeling and characterization of R-SP-A are discussed elsewhere (Ruano et al., 1997).

### Epifluorescence microscopy of LSE films

The LSE in chloroform/methanol (3:1, vol/vol) was mixed with 1 mol % of the fluorescent phospholipid probe NBD-PC in the same solvent, based on the phospholipid content of LSE. This was spread on the buffered saline subphase ( $\pm 5$  mM CaCl<sub>2</sub>) at an ambient temperature of  $23 \pm 1^\circ\text{C}$  to form solvent-spread LSE films in an epifluorescence microscopic surface balance whose design and performance is discussed elsewhere (Nag et al., 1990). In some experiments small amounts of fluorescently labeled TR-SP-A (0.13  $\mu\text{g}/\text{ml}$  final concentration) were dissolved in the subphase buffer and LSE films were solvent-spread on top of this subphase.

The solvent-spread LSE films were compressed at an initial rate of 9  $\text{\AA}^2/\text{molecule}/\text{min}$  in 20 or 50 steps. The LSE films were spread at an initial area per phospholipid molecule of 120  $\text{\AA}^2/\text{molecule}$ . Including both the total time for compression steps and for video recording, the effective overall quasistatic compression rates were 3.7 (fast, 32 min for complete compression) and 0.45 (slow, 4.4 h for complete compression)  $\text{\AA}^2/\text{molecule}/\text{min}$  (based on the phospholipid content of LSE), and the surface pressure-area per phospholipid ( $\pi$ -A) isotherms were recorded. The slow rate was chosen to observe any near-equilibrium features or shapes of condensed domains, such as typical kidney bean shapes observed previously in films of DPPC compressed at similar rates (Nag et al., 1991; Klopfer and Vanderlick, 1996). Compressions were stopped for 1–5 min at each of the 20–50 steps for visual observation and recording on videotape via a charge couple device (CCD) camera attached to the microscope (Nag et al., 1990). In some experiments the films compressed and expanded rapidly through 10 cycles at a rate of  $707 \text{ mm}^2 \cdot \text{s}^{-1}$  (292  $\text{\AA}^2/\text{molecule}/\text{s}$ ) and the 11th compression was then performed at the overall quasistatic compression rate of 3.7  $\text{\AA}^2/\text{molecule}/\text{min}$  during which video images were recorded. In some experiments TR-SP-A was dissolved in the subphase buffer of solvent-spread LSE (+1 mol % NBD-PC) films and the fluorescence was observed from either the lipid probe or the labeled protein by switching filters using methods discussed elsewhere (Nag et al., 1996; Ruano et al., 1998). The recorded images were digitally processed and analyzed using an image analysis program JAVA 1.3 (Jandel Scientific, San Rafael, CA). An average of 10 randomly selected frames were analyzed at various surface pressures by methods discussed elsewhere (Nag and Keough, 1993). The total amount of condensed phase was calculated and expressed as percentage of the total film by dividing the total amount of black or probe excluding regions per frame by the total area of each frame  $\times 100$  (Nag and Keough, 1993).

The recorded images were digitally processed and analyzed using the image analysis program JAVA 1.3 (Jandel Scientific, San Rafael, CA). Quantitation was done after contrast enhancement using the enhancement menus of the software. For certain images above 50 mN/m definition between regions was low, and so quantitation was not attempted.

### Adsorbed LSE films

Appropriate amounts of LSE in chloroform:methanol (3:1, vol/vol) were dried in chromic acid-cleaned glass vials under a steady stream of N<sub>2</sub> to

form dried layers at the bottom of the vials, and the vials were evacuated overnight. Suspensions of the dried material were formed by vortexing the films in buffer to give vesicular LSE suspensions. The suspensions were injected under the air-buffer interface in a modification of the epifluorescence microscopic balance to observe adsorption, the design of which is discussed elsewhere (Nag et al., 1996b). Adsorption of LSE suspensions was monitored by the NBD-PC fluorescence from the adsorbed films formed at the air-buffer interface, and the images were observed and recorded every 15 min for 4 h.

## RESULTS AND DISCUSSION

### Phase transitions in LSE films

A typical compression isotherm and images observed from a film of LSE plus 1 mol % NBD-PC on a buffered saline

subphase (without calcium) are shown in Fig. 1. The  $\pi$ -A isotherm indicated a lift-off at  $120 \text{ \AA}^2/\text{molecule}$  and a plateau region at a surface pressure near  $45 \text{ mN/m}$ . The images observed indicated that at a low surface pressure of  $\sim 5 \text{ mN/m}$  the monolayer was homogeneously fluorescent (A). The liquid condensed or probe excluding (black) domains appeared at  $\pi$  near  $13 \text{ mN/m}$ , grew in size (B and C) with increasing  $\pi$ , and then decreased in size at  $\pi$  above  $40 \text{ mN/m}$  (D). Above the plateau region of the isotherm at  $45 \text{ mN/m}$ , the discrete condensed domains mostly disappeared, leading at first sight to apparent reductions in the total dark region. However, the distribution of light and dark monolayer fluorescence became different than at lower  $\pi$ , and the film acquired an appearance of thin black filamentous re-

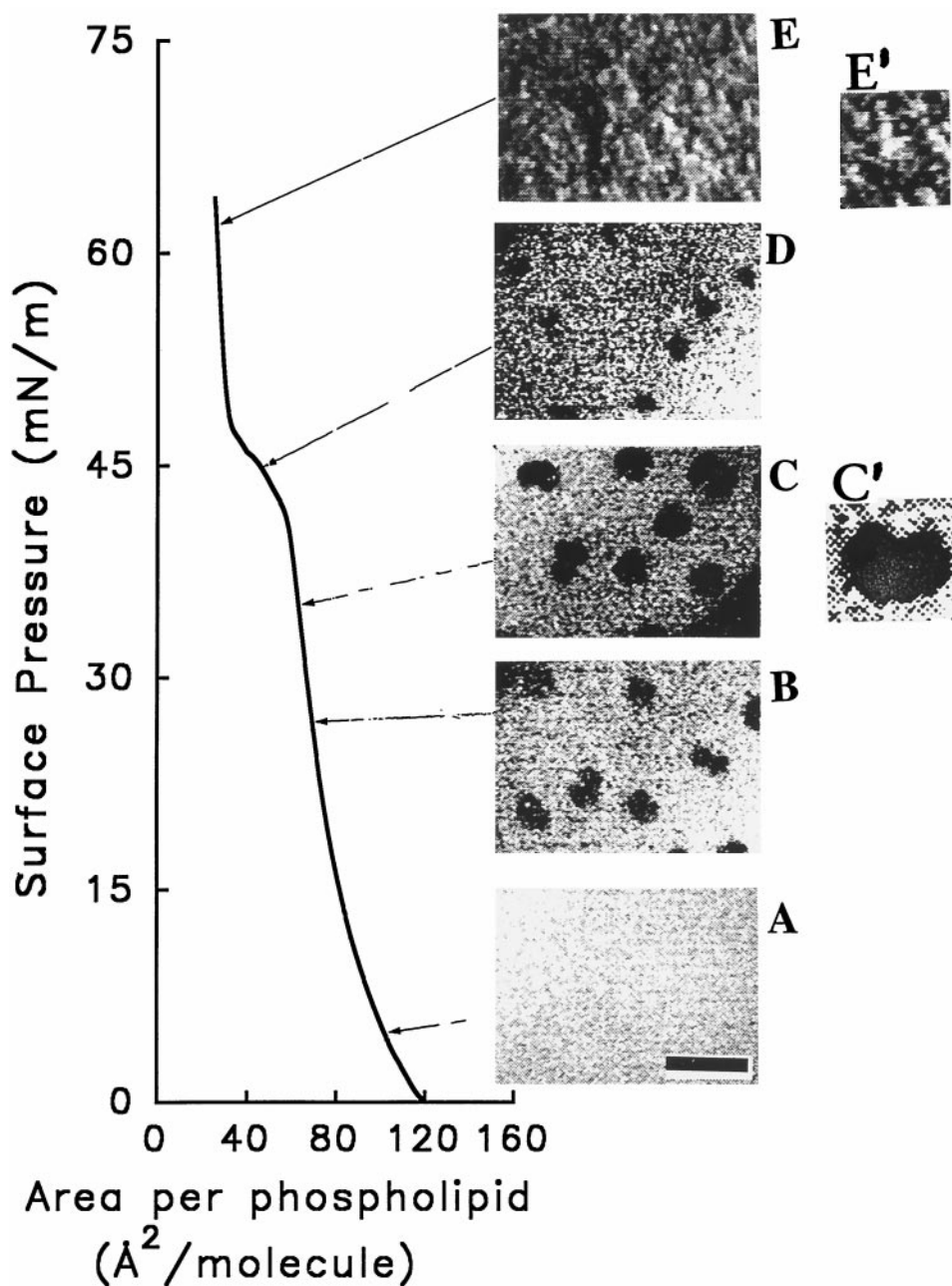


FIGURE 1 Isotherms and images of LSE monolayers. Surface pressure-area per phospholipid molecule ( $\pi$ -A) isotherm of porcine LSE + 1 mol % NBD-PC and the typical images (A-E) obtained from such films at surface pressures indicated by arrows in the isotherms. The films were spread from organic solvents onto an air-buffer (150 mM NaCl, 5 mM Tris-HCl, pH 6.9) interface at a temperature of  $23 \pm 1^\circ\text{C}$ , and compressed at a rate of  $0.45 \text{ \AA}^2 \cdot \text{molecule}^{-1} \cdot \text{min}^{-1}$  in 50 steps. The black regions in the images (A-E) indicate the liquid condensed phase and the white regions the fluorescent probe containing liquid expanded phase. The scale bar is  $25 \mu\text{m}$  for A-E. The images in C' and E' are enlarged ( $\times 3$ ) views of a part of C and E.



gions coexisting with regions of intense fluorescence. The filaments were extremely thin ( $\sim 1 \mu\text{m}$ ) and almost beyond the optical resolution of the fluorescence microscope. Because of the signal to noise in the images, quantitation of black phase was not attempted. Images such as those as in (*E*) were difficult to observe and video record, since the new distribution of fluorescent probe decreased the resolution between the black and fluorescent regions (magnified view of *E* shown in *E'*). These features indicated that a liquid expanded (LE) to liquid condensed (LC) phase transition occurred in porcine LSE films, and had features similar to those seen in films of calf LSE films (Discher et al., 1996). The redistributed morphology seen at higher magnifications at higher pressures did not seem to be observed by Discher et al. (1996). Whether this difference is a matter of resolution or some more fundamental aspect of the two sets of observations is not yet known.

The images seen at intermediate  $\pi$  in Fig. 1, *B* and *C* showed condensed domains (black), some of which had kidney bean shapes (an enlarged view of such a domain is shown in *C'*). Such kidney-shaped domains were previously observed in DPPC films compressed under quasiequilibrium conditions (Flörshheimer and Möhwald, 1989; Nag et al., 1991; Weis, 1991). Their appearance suggests, but does not confirm, that the condensed domains in LSE films may be made of, or at least rich in, DPPC. Recent calculations performed on the amounts of condensed phase in spread films of calf LSE films indicated that there was a direct proportionality of the amount of DPPC present in calf surfactant with the highest amount of condensed phase found in such films (Discher et al., 1996). This evidence would tend to suggest that the condensed domains of porcine LSE films may be made of the main component of surfactant, DPPC. Some of the phase transition features of LSE films, such as the appearance and disappearance of condensed domains with increasing  $\pi$ , have also been reported previously in films of calf lung surfactant extracts (CLSE) using epifluorescence and Brewster angle microscopy (Discher et al., 1996), and in films of DPPC/DOPC using fluorescence microscopy (Nag and Keough, 1993). In the previous study we had attributed the decrease of condensed phase at high  $\pi$  in films of DPPC/DOPC (plus NBD-PC), to the repartitioning of the probe at higher  $\pi$  (Nag and Keough, 1993). The Brewster angle microscopy study by Discher et al. (1996) (which did not require fluorescent probes) suggests that these features of domain distributions in films of lung surfactant extracts, and possibly in the simpler model system, are intrinsic properties of the phase transitions in such films. As noted below, at very high pressures the film takes on a new appearance of a finely divided black and fluorescent meshwork. Should such a transition be occurring in the films around 45 mN/m, resolution limitations might, however, cause an overestimation of fluorescent phase.

The appearance of the finely divided material of dark and light domains at higher pressures suggests that yet another transformation of the film occurs above pressures of  $\sim 45$

mN  $\cdot$  m<sup>-1</sup> (Fig. 1, *E* and *E'*). This network is reminiscent of that seen by Hwang et al. (1995) in DPPC and DPPC/cholesterol films at high surface pressure using near-field scanning optical microscopy.

The frequency distributions of condensed domains for relatively fast (3.7 Å<sup>2</sup>/molecule/min) and slow (0.45 Å<sup>2</sup>/molecule/min) compression of LSE films at comparable  $\pi$  are shown in Fig. 2 *a*. The patterns in Fig. 2 *a* indicated a difference in the distribution of the condensed domain sizes for the two systems. For example, in the film compressed at the faster rate the average sizes of condensed domains were  $\sim 40$  square  $\mu\text{m}^2$  at 28 mN/m, whereas in the slowly compressed one at the same  $\pi$ , the average size was 120  $\mu\text{m}^2$ . The distributions also indicate that in case of the fast compression, greater numbers of smaller condensed domains were formed compared to the slowly compressed films. Also, the dispersion of sizes of the condensed domains in the case of the fast compression was smaller at all  $\pi$  compared to those of slowly compressed films. A similar pattern of the effect of compression rate on condensed domain distribution has been previously reported for films of DPPC and other phospholipids (Helm and Mowald, 1988; Nag et al., 1991; Klopfer and Vanderlick, 1996).

Fig. 2 *b* shows the average size (*A*), number (*B*), and total amount of black or condensed phase (*C*) plotted as a function of  $\pi$  for LSE films compressed at slow and fast rates. As noted above, compared to the faster rate the domain sizes were larger and their numbers lower in the films compressed at the slow rate. However, the total amount of condensed phase was similar in both systems (*C*). This fact suggested that the condensed (black) regions in LSE films were phase structures formed due to the process of a two-dimensional phase transition and the resulting phase was independent of the conditions (compression rates) used to transit from one phase to the other. As noted the total amount of condensed phase decreased at  $\pi$  above 30 mN/m, a property observed in films of DPPC/DOPC (Nag and Keough, 1993) and in films of CLSE (Discher et al., 1996). It is likely that the dark domains in the films of LSE are enriched in or nearly pure DPPC as suggested by Discher et al., 1996. With the exception of DPPG, a minor component of LSE, DPPC is the only component lipid that to our knowledge forms the kidney-shaped domains. Given the complex composition, however, and the fact that the shapes are a function of a balance of line tension and dipole density, assignment of the dark domain composition is not unequivocally possible.

The ordered or condensed domains observed in the porcine LSE films studied here support the idea that a fluid-to-ordered transition occurs in pulmonary surfactant films with increasing surface pressure or packing density and is similar to the ones observed in films of calf LSE (Discher et al., 1996). From early studies on the thermotropic phase transitions of pulmonary surfactant or its lipid extracts (LSE) in bilayer, it was suggested that the principal component of the surfactant responsible for an ordered-to-fluid transition during heating was DPPC (Träuble et al., 1974).

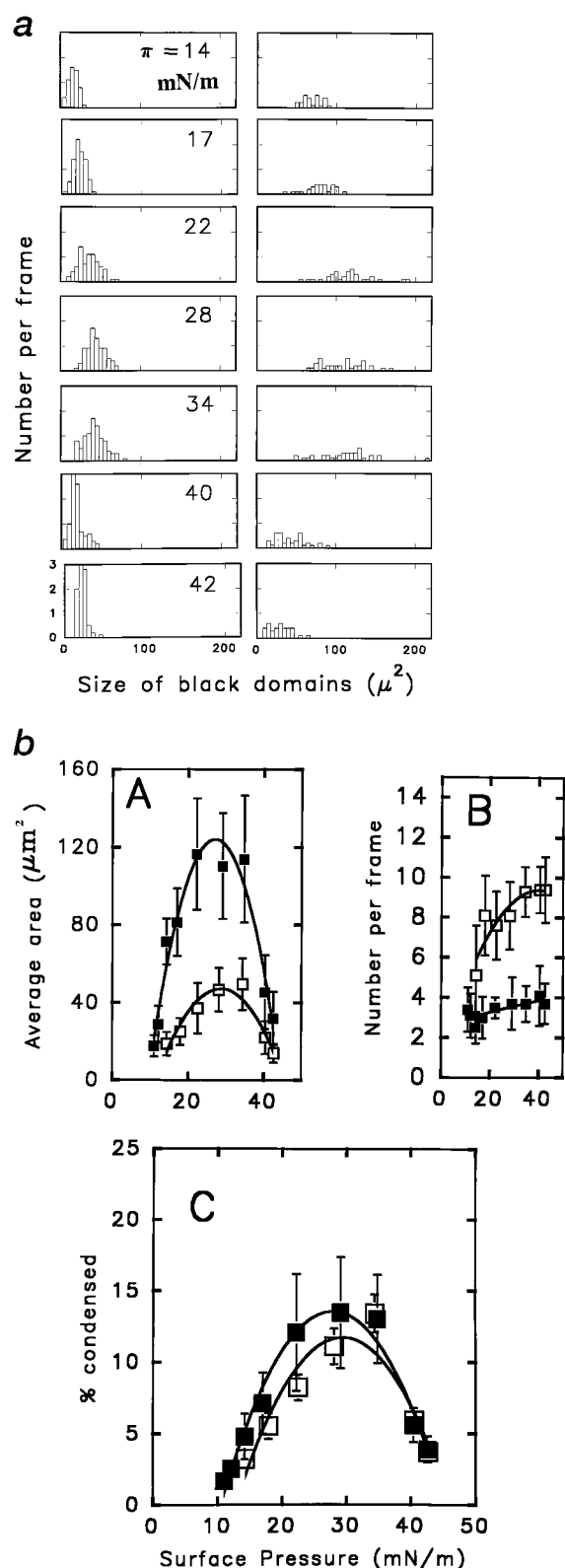


FIGURE 2 Distribution of domains in LSE films. (a) Frequency distribution of sizes of condensed (black) domains seen in LSE films compressed at relatively fast 3.7 (left) and slow 0.45 (right)  $\text{\AA}^2 \cdot \text{molecule}^{-1} \cdot \text{min}^{-1}$  rates. (b) The average size (A), number (B), and total amount (C) of condensed phase domains obtained from the two types of films. The numbers in each panel in a indicate the surface pressures in mN/m, where the images were obtained. (b) Slow (solid symbols) and fast (open symbols)

Others have detected that the “squeeze-out” plateau and surface compressibility of canine surfactant films changes abruptly over a temperature range of 30–35°C (King and Clements, 1972). Electron paramagnetic resonance (EPR) studies of rabbit surfactant suspensions have suggested that the material is mainly fluid at room temperature, and the fluidity was of the material imparted by the presence of a significant amount of unsaturated lipids in such material (Hook et al., 1984). EPR probes are known to preferentially partition into fluid regions in bilayers containing mixtures of fluid and rigid lipids (Oldfield et al., 1972). Others have indicated by differential scanning calorimetry (DSC) of rabbit surfactant suspensions that the material is partly fluid at 37°C and not very fluid at room temperature (Keough et al., 1985). Dluhy et al. (1989), using infrared spectroscopy of surfactant suspensions and films, have indicated that a continuous decrease of the  $\text{CH}_2$  stretching frequency of the C—C bonds of the acyl chains of surfactant lipids occurred with increased packing of such films. They also showed that in highly compressed bovine surfactant films ( $>30$  mN/m), most of the phospholipid chains were in an all *trans* configuration (Dluhy et al., 1989).

The functional significance of condensed domains in films of pulmonary surfactant is not clear in the alveoli, but an interesting proposition has been put forward by Bangham (1987; see also Keough, 1992). This proposition is based on the observations that the surfactant film in the lung alveoli is almost made of condensed or “solid lipids,” or DPPC. Such films can have regions or “solid islands” existing in a “sea” of fluid lipids (Bangham, 1987). The solid lipid regions act as “splints” in the alveolar wall, and prevent them from collapsing with decreasing alveolar wall area or volume (Bangham, 1987). Such splinting would occur if each of the alveoli is considered as a “geodesic dome” or a dodecahedron or the inside surface made of many small flat surfaces, where each side of the alveolar wall would provide a surface on which such splints reside (Bangham, 1987). The finely divided black (solid) and white (fluid) network is reminiscent of a metal alloy. If such a “two-dimensional alloy” existed in the film at high pressure, then it might impart to the film strength and moderate flexibility simultaneously. Such characteristics could be of special significance to lung stability at low volumes, and under conditions of lung movements and dynamic volume changes. Whether the condensed domains or the solid latticework in LSE films could fulfill the properties of such “splints” or “alloys” in situ in the alveoli remains speculative, but provocative.

#### Adsorbed LSE films

Typical isotherms and images of adsorbed LSE films formed by injecting LSE suspensions containing 1 mol % of

rates of compression. The data were obtained by analyzing 10 randomly chosen frames at each surface pressure. The error bars indicate  $\pm$  one standard deviation.

fluorescent probe NBD-PC under a film-free air-buffer interface are shown in Fig. 3. Formation of the film and changes in its morphology with time were observed via the fluorescence of the lipid probe. When injected at a concentration of 0.06 mg/ml, the material increased the surface pressure of the air-buffer interface in a few minutes to 45 mN/m. The typical image (D) observed at 45 mN/m showed a phase of low fluorescence plus regions of aggregated probe. When material was injected at a lower concentration of 0.006 mg/ml (*bottom*) the surface pressure increased

relatively rapidly to 13 mN/m and then more slowly. At 13 mN/m the adsorbed films had the appearance of an almost homogenous fluid phase, with small, barely visible condensed domains (A). More condensed domains appeared at higher pressures, increasing in number and size (B and C) over a 4.5 h period of further adsorption up to a  $\pi$  of 24 mN/m. Films could not be observed for longer times presumably because the fluorescence probes photobleached over that period of time. These observations suggested that the process of an expanded-to-condensed phase transition

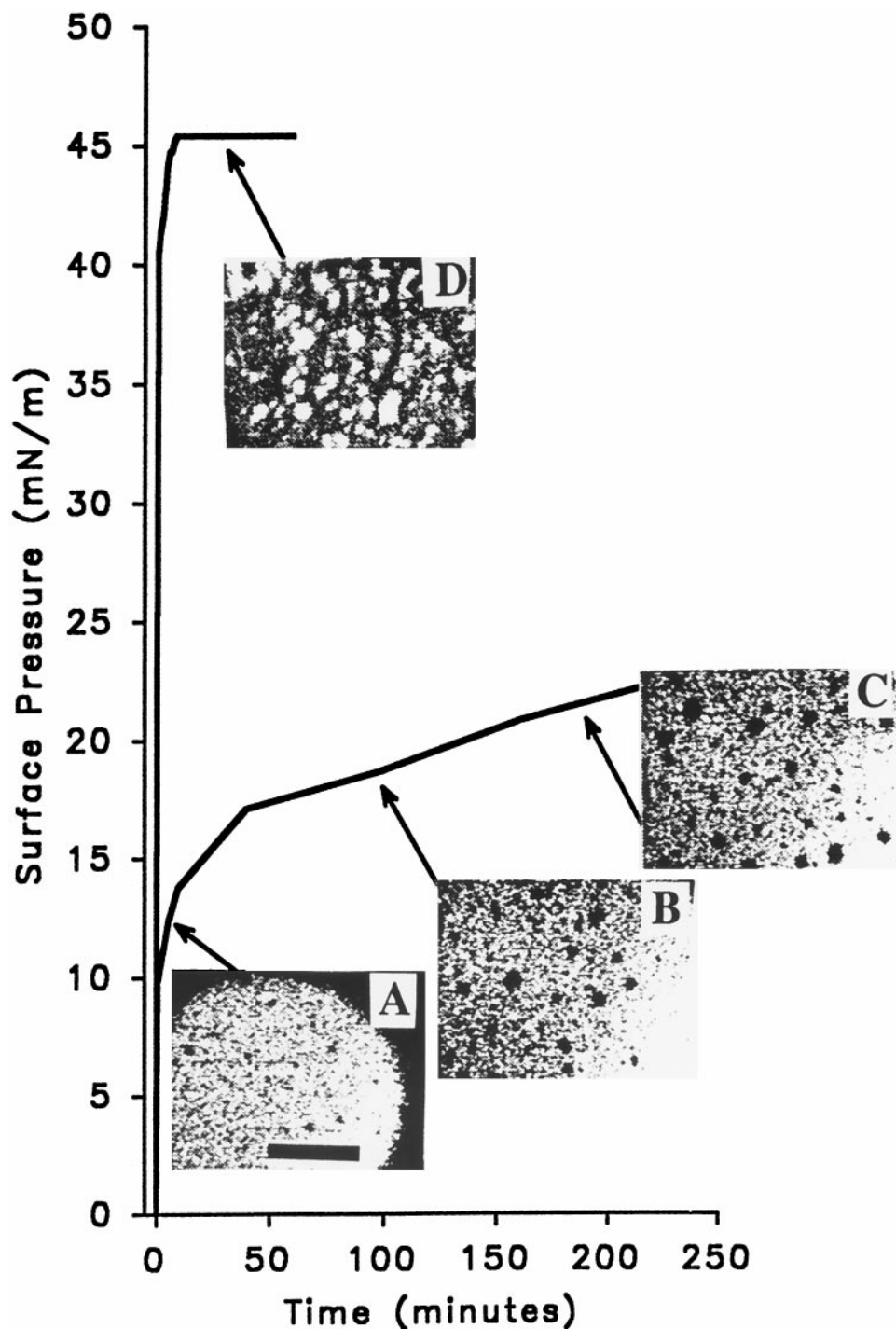


FIGURE 3 Images of adsorbed LSE films. Typical surface pressure-time ( $\pi$ - $t$ ) isotherms and images of LSE + 1 mol % of NBD-PC adsorbed films formed by injecting 0.06 mg/ml (*top*) and 0.006 mg/ml (*bottom*) under an unstirred air-buffer interface. The typical images observed in such films are indicated by letters A-D, and the  $\pi$  where they were obtained by arrow marks in the isotherms. The black regions represent the condensed phase and the bright regions the fluorescent or expanded phase. A smaller amount of LSE suspension was injected under the buffer (*bottom*), to obtain a slowly adsorbed sample. Scale bar is 25  $\mu$ m.

seen in spread LSE films with compression (Fig. 1) also occurred in adsorbed LSE films as packing density increased as materials adsorbed into the surface film.

The size of the condensed domains in the adsorbed films were smaller than those seen in the solvent-spread LSE film (Fig. 1), since the adsorbed films were initially more rapidly compressed ( $\pi > 15$  mN/m in 30 min) than their solvent-spread counterparts ( $\pi \sim 15$  mN/m was reached after 2 h). Previous studies indicated that solvent-spread and adsorbed DPPC and DPPC/SP-C films were similar at equivalent packing densities and that condensed domains were smaller in more rapidly adsorbing DPPC/SP-C films than in the slowly formed films of lipid alone (Nag et al., 1996b). This effect appears to be equivalent to the solvent-spread DPPC films whose rapid compression yields smaller and more numerous condensed domains in comparison to those undergoing slow compression (Nag et al., 1991; Klopfer and Vanderlick, 1996). The appearance of smaller condensed domains during rapid compression or adsorption of a film in comparison to fewer larger domains in their slowly formed counterparts likely occurs because of a balance of diffusion-limited domain growth with an increase in nucleation sites in order to meet the requirement for a given total amount of solid phase at any  $\pi$  (Nag et al., 1991). The hydrophobic proteins and unsaturated lipid components of LSE promote the rate of adsorption of lipid over adsorption of simple films such as DPPC. These studies indicate that adsorbed and spread films of LSE appear to be equivalent as with the simpler films of DPPC and DPPC/SP-C (Nag et al., 1991; Klopfer and Vanderlick, 1996). At present, instrumental limitations prohibit us from studying adsorbed films of LSE under dynamic compression-expansion cycling.

### Dynamic cycling and squeeze-out from LSE films

The  $\pi$ -A isotherm of a LSE film spread at a initial  $\pi$  of 35 mN/m dynamically compressed and expanded 11 times, and typical images seen at  $\pi \sim 25$  mN/m from the first (A) and 11th (B) compression are shown in Fig. 4 a. The 11th compression was obtained at a slow rate. In Fig. 4 b the number (A), size (B), and total amount (C) of condensed domains, plotted as a function of  $\pi$  from the 11th compression (Fig. 4 a) compared to those from a separate LSE film compressed once at the same rate as in Fig. 1, are shown. The images in 4 a indicated that the number of condensed domains were increased at 35 mN/m in the 11th cycle compared to the ones seen after initial spreading of the film at a  $\pi$  of 35 mN/m. The total amount and number of domains were also increased at equivalent  $\pi$  during the 11th compression compared to the films compressed only once. At all surface pressures the amount of condensed phase in the 11th compression was about 3–5% higher than those seen in films compressed once (data obtained from two independent experiments). Because the change is so small it only becomes apparent after a fairly large number of cycles. This increase in condensation suggests that the amount of

the material forming the black or condensed domains in LSE films (presumably DPPC) increased in the surface films upon dynamic cycling of such films. Some selective exclusion of fluid materials such as unsaturated lipids or proteins that inhibit the formation of condensed domains may have occurred on repetitive cycling, as seen in previous studies with DPPC/unsaturated-PC films (Nag and Keough, 1993). These results tend to support assumptions that fluidizing components of surfactant are squeezed out or lost upon dynamic cycling of surfactant in the alveoli, eventually refining and enriching the films with DPPC (Goerke and Clements, 1986; Keough, 1992). An alternate explanation for the increase in condensed domains could be some change in packing efficiency after repetitive cycling. This would have the same net effect in the lung.

In lungs at low volume the surface tension of the air-alveolar fluid interface is near 0 mN/m (Schürch et al., 1976), and the only major component of surfactant that can reach such low values upon compression is DPPC (Goerke and Clements, 1986; Keough, 1992; Pison et al., 1996). Studies in vitro and in situ on the surface activity of pulmonary surfactant have suggested that the material near an air-water interface shows a variety of complex phenomena, such as molecular adsorption-desorption, squeeze-out, spreading-respreading, and that some combination of all these processes is likely involved in achieving lung stability in situ (Otis et al., 1994; Pison et al., 1996; Scarpelli and Mautone, 1994; Yu and Possmayer, 1993; Clements, 1977; Bachofen et al., 1987; Schürch et al., 1985, 1992a). These and other studies of dynamic cycling of pulmonary surfactant have suggested that the surface films are enriched in DPPC, and the enrichment probably occurred by loss of components unable to reach low surface tension (Gross, 1995) or the selective adsorption of the components such as DPPC (Schürch et al., 1992a; 1994). Schürch et al. (1992a; 1994) have suggested that adsorbed surfactant films have a reservoir or pool of lipids under the surface film that enriches the surface with DPPC, and that SP-A and calcium enhance the adsorption of DPPC to the surface (Schürch and Bachofen, 1995). Since the LSE films studied here in the dynamic cycling experiment were spread from solvent, and there was no SP-A or calcium present in these experiments, only limited reinsertion of materials from the excluded and collapse phases might have occurred.

### Interactions of LSE films with calcium

A  $\pi$ -A isotherm of a slowly compressed LSE film (plus 1 mol % NBD-PC) on a buffered subphase containing 5 mM calcium and the typical images observed in such a film with increasing  $\pi$  (indicated by arrows in the isotherms) are shown in Fig. 5 a. The number (A), size (B), and amount (C) of condensed domains plotted as a function of  $\pi$ , compared to the ones without calcium, are shown in Fig. 5 b. Although the isotherm of the LSE-Ca film in Fig. 5 a is not significantly different from the one without calcium (Fig. 1), the



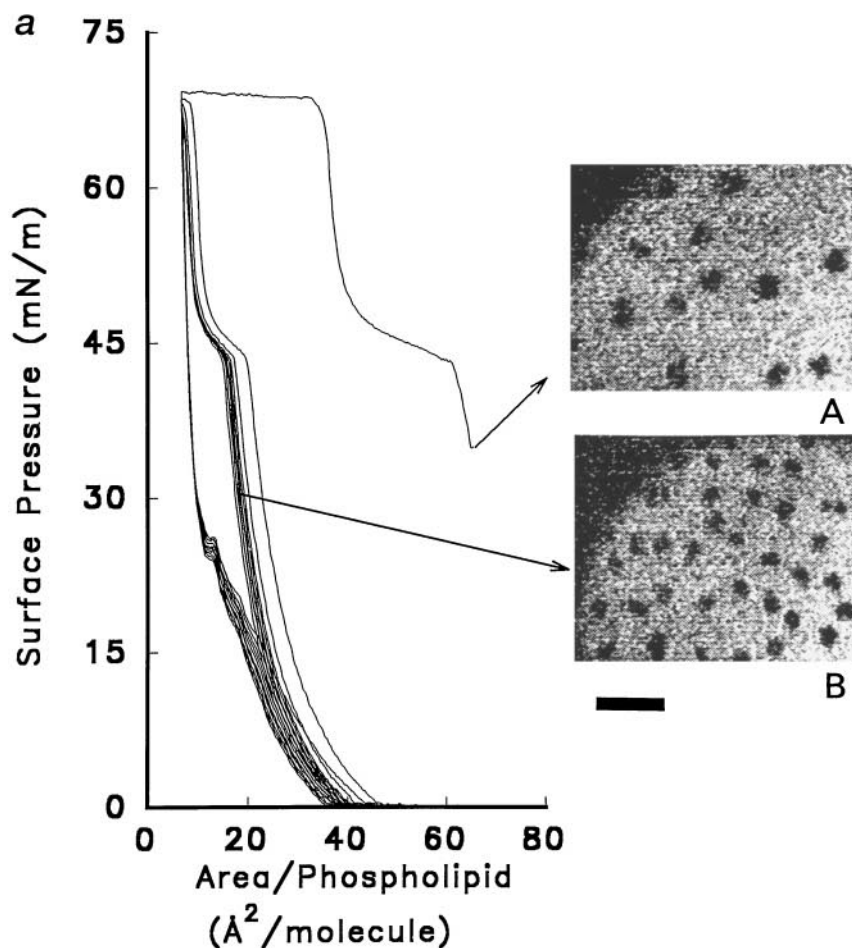
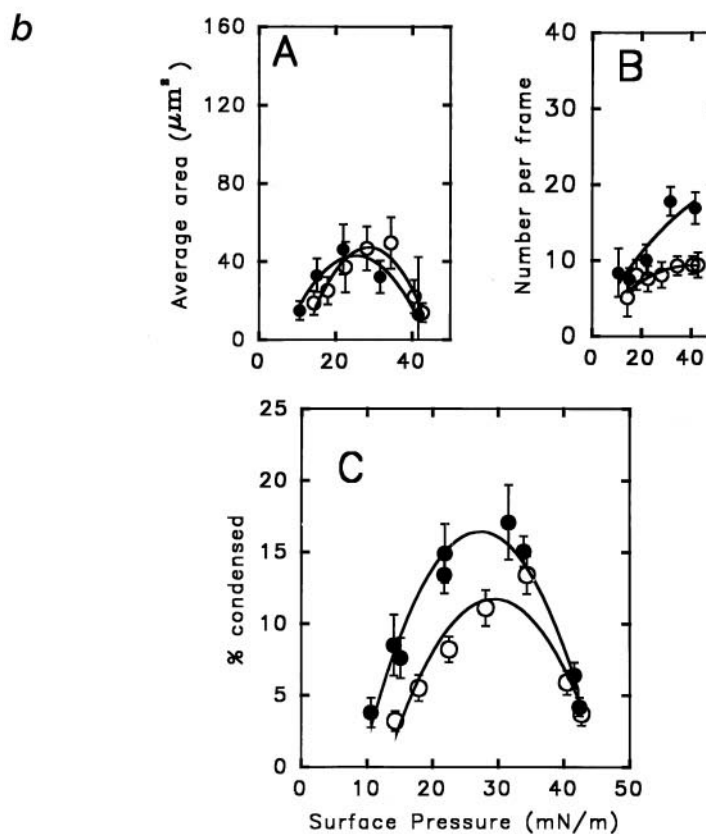


FIGURE 4 Repetitive compression and expansion of LSE films. Typical  $\pi$ -A isotherms of a LSE film compressed and expanded rapidly for 10 times (at a rate of  $707 \text{ mm}^2 \cdot \text{s}^{-1}$ ) and slowly ( $20 \text{ mm}^2 \cdot \text{s}^{-1}$ ) for the 11th time, and the typical images observed at a  $\pi$  of 35 mN/m in the initially spread film (A) and in the 11th compression (B) are shown in (a). The scale bar is  $25 \mu\text{m}$ . (b) The size (A), number (B), and total amount (C) of condensed phase estimated from the first (*open symbols*) and the 11th (*closed symbols*) compression of two LSE films plotted as a function of  $\pi$ . The standard deviations are for 10 randomly selected images analyzed at each  $\pi$ .





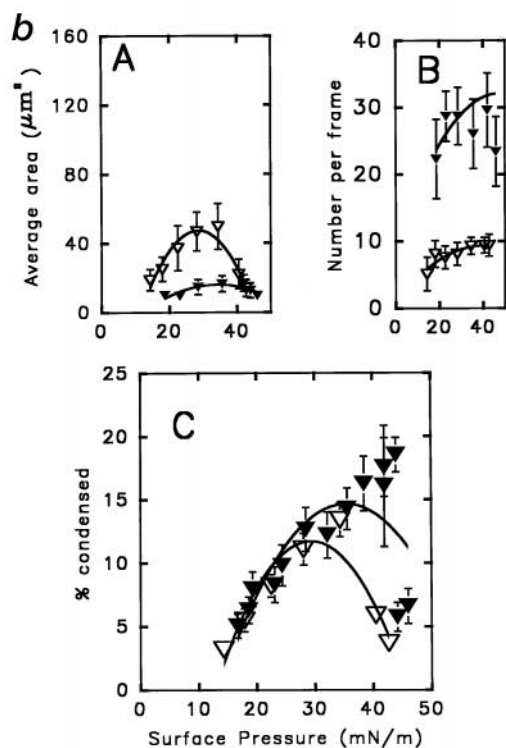
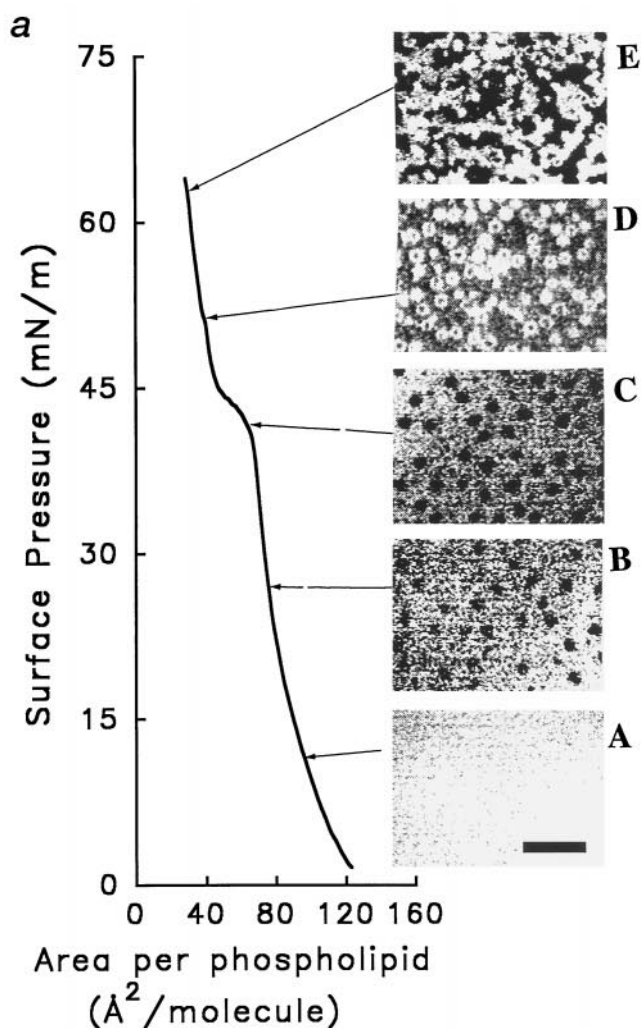


image analysis data indicated that formation of condensed phase in such films was somewhat different from ones in the absence of the cation. The sizes of condensed domains (Fig. 5 *b*, *B*) in the LSE-Ca films were smaller, and their shapes more circular than the larger kidney-shaped domains observed in films without calcium (Fig. 1, *A* and *C*). The total amount of condensed phase was also higher at  $\pi$  between 35 and 45 mN/m in LSE-Ca films compared to the films without the cation (Fig. 5 *b*, *C*). At  $\pi$  above 40 mN/m, the LSE-Ca films had bright circular regions or fluorescent (white in the figure) domains dispersed in a background of dull fluorescent phases. These white regions or domains also had small black centers (images *D* and *E* in Fig. 5 *a*). At higher  $\pi$  ( $>45$  mN/m) the total amount of condensed phase also decreased in the LSE-Ca films, a pattern similar to the ones seen in films without the cation, although the value of  $\pi$  up to which the amount of condensed domains increased in LSE-Ca films was higher than in films without calcium. The total amount of condensed phase and their shapes in LSE-Ca films were similar to the ones observed by Discher et al. (1996) in calf LSE films with calcium. In films of DPPC/DPPG (7:3 mol/mol), we observed that 2 mM calcium caused an increase in the amount of condensed phase and a change of shapes of condensed domains compared to films without the cation (Nag et al., 1994).

The fluorescent aggregates (Fig. 5 *a*, *D* and *E*) observed in LSE-Ca films at higher  $\pi$  were absent in films without the cation (Fig. 1, *D* and *E*). Above  $\pi$  of 45 mN/m the low fluorescence field might suggest the presence of a condensed or solid-like phase that contains a small amount of probe, it perhaps being somewhat different from the standard condensed phase. The rearrangements at the high  $\pi$  could be an indication of phase segregation of acidic lipids by calcium.

The amount of condensed phase observed in the presence of calcium between  $\pi$  of 35–45 mN/m was greater than in films without calcium. As some of the PG in surfactant is likely saturated (DPPG), its aggregation in DPPG- or DPPC/DPPG-rich phases may be responsible for this observation. This factor, plus the fact that the domains in such films in the presence of calcium did not have the typical kidney shape of DPPC domains, may suggest that with the higher calcium concentration used here (5 mM) the domains

FIGURE 5 Effect of calcium on LSE films. (a) Surface pressure-area per phospholipid molecule ( $\pi$ -A) isotherm of LSE + 1 mol % NBD-PC films spread on a buffered subphase containing 5 mM calcium, and the typical images (A–E) obtained from such films at  $\pi$  indicated by arrows in the isotherm (all other conditions were the same as in Fig. 1). (b) Size (A), number (B), and total amount (C) of the condensed (black) phase observed in such films with (closed symbols) and without (open symbols) calcium. The black regions of the images (A–C) in (a) indicate the condensed phase and the white ones the fluorescent-probe containing expanded phase. In *D* and *E* the white regions represent calcium-induced probe containing domains. The scale bar is 25  $\mu$ m. An average of 10 frames were analyzed from two different films at each  $\pi$  in (b). The error bars indicate  $\pm$  one standard deviation.

may not be totally made of DPPC, as suggested by Discher et al., (1996).

A number of previous studies have indicated that ionic and hydration conditions determine the morphology and functional properties of pulmonary surfactant (Goerke and Clements, 1986; Keough, 1992). Effects of calcium have been observed on surfactant morphology and tubular myelin formation in the bulk phase (Benson et al., 1984) on ability to reach low surface tension on compression (Amirkhanian and Merrit, 1995; Amirkhanian and Taesch, 1993; Haddad et al., 1994), adsorption (Efrati et al., 1987), and on thermotropic properties (Mautone et al., 1987; Ge et al., 1995). This study of LSE-Ca films supports previous findings that implicate sensitivity of surfactant to electrostatic interactions caused by calcium. Morphological differences are induced in the monolayers that are also partially reflected in bilayer forms of surfactant. The rearrangement of components under the influence of calcium likely has important consequences for surfactant dynamics.

At higher surface pressures ( $>45$  mN/m) in LSE films, the appearance of heterogeneous irregular probe distribution

and the decrease of observable condensed phase might indicate that the phase in LSE films is not a simple liquid condensed (LC) phase. The changes in the LSE films compared to those of DPPC can be due to the effect of unsaturated lipids, cholesterol, and the hydrophobic proteins SP-B and SP-C on film packing. Hall and co-workers have suggested that the amount of cholesterol or neutral lipids of surfactant may be the main deciding factor controlling the size and amounts of condensed domains of lung surfactant films (Hall et al., 1995; Discher et al., 1996).

### Interaction of SP-A with LSE films

Films of LSE were spread from solvents and compressed on a buffered subphase containing fluorescently labeled R-SP-A. Typical images observed in such LSE films at a  $\pi$  of 35 mN/m with subphase containing  $0.13 \mu\text{g/ml}$  of fluorescently labeled SP-A are shown in Fig. 6. The top panels (A and B) were obtained without calcium, and the bottom ones (C and D) in the presence of calcium. The images on the left

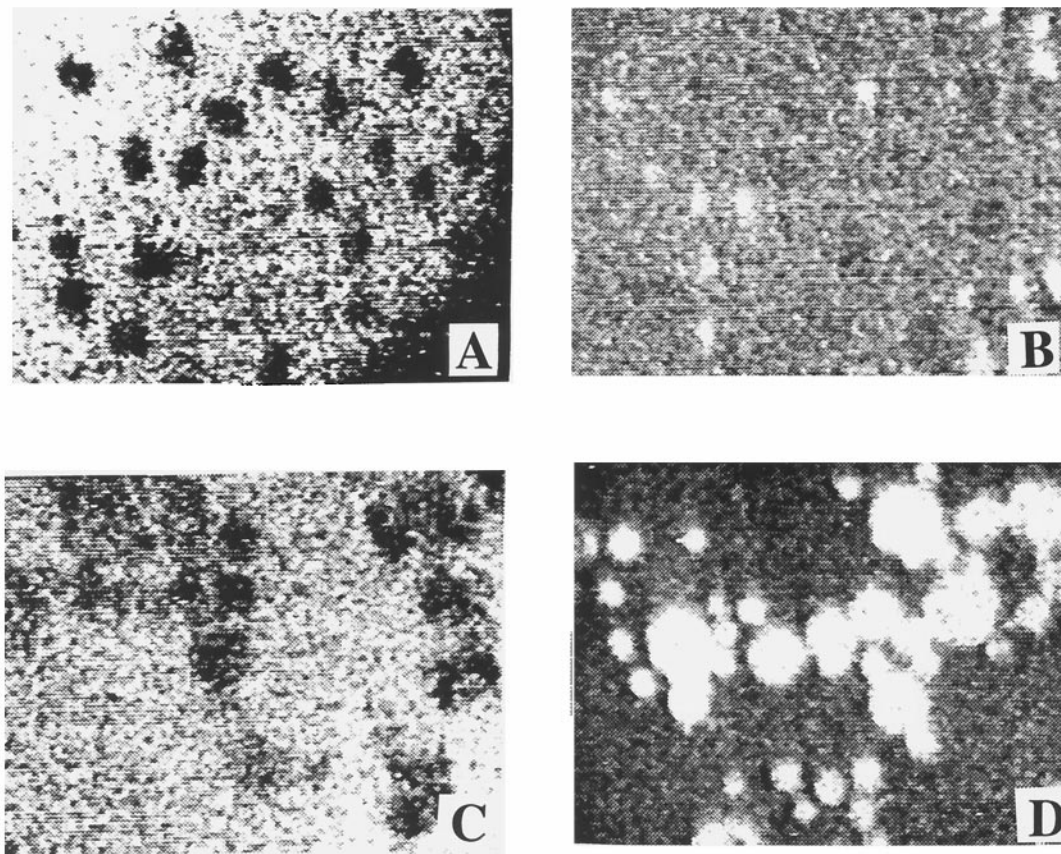


FIGURE 6 Effect of calcium on lipid and SP-A domains. Typical images observed at  $\pi$  of 35 mN/m in films of LSE + 1 mol % NBD-PC spread over containing  $0.13 \mu\text{g/ml}$  R-SP-A on a buffered subphase without (A and B) and with (C and D) 5 mM calcium. The images on the left (A and C) were observed from the fluorescence of NBD-PC and those on the right (B and D) from that of R-SP-A. The black regions on the left panel represent the condensed phase, and the bright areas the expanded phase. The bright regions in the right panel represent the fluorescence from R-SP-A inserted in or very close to the LSE films. The scale bar is 25  $\mu\text{m}$ .



(A and C) were observed from the fluorescence of NBD-PC, and the ones in the right (B and D) from the fluorescence of R-SP-A. The images indicated that SP-A inserts in LSE films or is in very close proximity to such films. Also, the images of the films in (C) indicated that SP-A in combination with calcium altered the distribution of condensed domains. The condensed domains were segregated into aggregates or regionalized, and such regions may have contained some protein (D). Panel D, observed from the fluorescence of the protein, also indicated that in case of the films containing calcium the protein R-SP-A aggregated into large domains. Aggregation of SP-A adsorbed onto DPPC/DPPG films under the presence of calcium was previously observed by Ruano et al. (1998). The appearance of the distribution of the TR-SP-A in the LSE films appears, however, somewhat different from that in the DPPC or DPPC/DPPG films.

Previous studies indicated SP-A may have interactions with surfactant lipids, and enhance the process of adsorption of the material into the air-alveolar fluid interface (Schürch et al., 1992b). Soluble SP-A also associated with lipids in surface films (Ruano et al., submitted for publication). These data indicate the SP-A inserted or adsorbed onto LSE films at low  $\pi$ , and in the presence of calcium the protein formed large aggregates or domains. The images such as in Fig. 6 C show that SP-A aggregated these condensed (dark) domains into clusters. This may be due to the binding of SP-A to the condensed lipid domains, since comparison of number of images shown in panels C and D indicated that the protein was localized in the vicinity or inside the clusters of the condensed domains. In a previous study of interaction of SP-A with DPPC films we found association of the protein with the boundaries of condensed lipids (domains), and aggregation of the protein into in condensed-fluid boundaries in DPPC/DPPG films (Ruano et al., 1998). In such simpler systems (plus or minus calcium), SP-A associated with the condensed domain boundaries only but did not aggregate the domains (Ruano et al., 1998). The difference of arrangement of SP-A in LSE films where lipid domain aggregation appears to be induced by SP-A may be due to the fact that LSE films contained other components such as the hydrophobic proteins, which possibly modify the influence of SP-A on the lipids.

Under certain conditions, SP-A binds selectively to the main component of lung surfactant, DPPC, and promotes phospholipid recycling into the type-II pneumocyte (Kuroki and Akino, 1991; Casals et al., 1993). It has been suggested that SP-A associates or binds to saturated or gel phase phospholipids (King et al., 1986; Casals et al., 1993). In combination with other surfactant proteins like SP-B and calcium, SP-A causes rearrangements of surfactant lipids, organizing bilayer multilamellar structures into tube-like bilayer structures called tubular myelin (Williams et al., 1991), a presumed precursor of the surface film in the alveoli. SP-A in combination with calcium is also known to extensively aggregate bilayer vesicles made of surfactant lipids (Efrati et al., 1987; Ruano et al., 1996). In this study

we found that interactions occurred between the condensed domains of LSE films SP-A and calcium. Since condensed domains of LSE films are made of saturated lipids such as DPPC, a specific interaction between such lipid or their gel-like phase with SP-A was likely to have occurred in LSE films also.

The studies here indicate that formation of condensed domains occurs in both spread and adsorbed film of porcine lung surfactant. The condensed phase of such films have structural similarities with the ones observed in films of DPPC, and the phase transition process is somewhat like that seen in films of simpler composition studied previously (Nag and Keough, 1993). Calcium and SP-A cause changes of the distribution of condensed domains in such films. The cycling of such films indicated small condensed phases of films of LSE could be slightly increased by dynamic cycling. These results allow for advances in our understanding of supramolecular morphology and its relation to surface activity in pulmonary surfactant enrichment of such films with DPPC.

We thank Lorne Taylor of Department of Chemistry, University of Waterloo, Ontario, for the MALDI analysis of the proteins.

This work was funded by grants from Medical Research Council of Canada (to K.M.W.K.), a NATO collaborative research grant (to K.M.W.K and J.P.G.), and grants from Fondo de Investigacion Sanitaria de la Seguridad Social and Comunidad de Madrid (to C.C. and J.P.G.). We also thank the School of Graduate Studies, Memorial University of Newfoundland, for financial assistance (to K.N.).

## REFERENCES

- Amirkhanian, J. D., and T. A. Merrit. 1995. The influence of pH on surface properties of lung surfactant. *Lung*. 173:243–254.
- Amirkhanian, J. D., and H. W. Tausch. 1993. Reversible and irreversible inactivation of preformed pulmonary surfactant surface films by changes in subphase constituents. *Biochim. Biophys. Acta*. 1165:321–326.
- Bachofen, H., S. Schürch, M. Urbenelli, and E. R. Weibel. 1987. Relationship among alveolar surface tension, surface area, volume, and recoil pressure. *J. Appl. Physiol.* 62:1878–1887.
- Bangham, A. D. 1987. Lung surfactant: how it does and does not work. *Lung*. 165:17–25.
- Bartlett, G. R. 1959. Phosphorous assay in column chromatography. *J. Biol. Chem.* 234:466–468.
- Benson, B. T., M. C. Williams, K. Sueshi, J. Goerke, and T. Sargeant. 1984. Role of calcium ions in the structure and function of pulmonary surfactant. *Biochim. Biophys. Acta*. 793:18–27.
- Bligh, E. A., and W. J. Dyer. 1959. A rapid method of total lipid extraction and purification. *Can. J. Biochem. Physiol.* 36:911–917.
- Casals, C., E. Miguel, and J. Perez-Gil. 1993. Tryptophan fluorescence studies on the interactions of surfactant protein A with phospholipid vesicles. *Biochem. J.* 296:585–593.
- Clements, J. A. 1977. Function of the alveolar lining. *Am. Rev. Resp. Dis.* 115:67S–71S.
- Discher, B. M., K. M. Maloney, W. R. Scheif, D. W. Grainger, V. Vogel, and S. B. Hall. 1996. Lateral phase separation in interfacial films of pulmonary surfactant. *Biophys. J.* 71:2583–2590.
- Dluhy, R. A., K. E. Reilly, R. D. Hunt, M. L. Mitchell, A. J. Mautone, and R. Mendelsohn. 1989. Infrared spectroscopic investigation of pulmonary surfactant. Surface film transition at the air-water interface and bulk phase thermotropism. *Biophys. J.* 56:1173–1181.

- Efrati, H., S. Hawgood, M. C. Williams, K. Hong, and B. T. Benson. 1987. Divalent cation and hydrogen ion effects on the structure and surface activity of pulmonary surfactant. *Biochemistry*. 26:7986–7993.
- Flörsheimer, M., and H. Möhwald. 1989. Development of equilibrium domain shapes in phospholipid monolayers. *Chem. Phys. Lipids*. 49: 231–241.
- Ge, Z. C. W., C. W. Brown, J. G. Turcotte, F. Wang, and R. H. Notter. 1995. FTIR studies of calcium-dependent molecular order in lung surfactant and surfactant extract dispersions. *J. Colloid Interface Sci.* 173: 471–477.
- Goerke, J., and J. A. Clements. 1986. Alveolar surface tension and lung surfactant. In *Handbook of Physiology—The Respiratory System III, Mechanics of Breathing*. P. T. Macklem and J. Mead, editors. American Physiological Society, Washington, DC. 247–261.
- Gross, N. J. 1995. Extracellular metabolism of pulmonary surfactant. The role of a new serine protease. *Am. Rev. Physiol.* 57:135–150.
- Gulik, A., P. Tchoreloff, and J. Proust. 1994. A conformation transition of lung surfactant lipids probably involved in respiration. *Biophys. J.* 67: 1107–1112.
- Haddad, L. Y., B. A. Holm, L. Hlavaty, and S. Matalon. 1994. Dependence of surfactant function on extracellular pH: mechanisms of modification. *Am. J. Physiol.* 76:657–772.
- Hall, S. B., K. Maloney, B. Korcakova, D. W. Grainger, W. Scheif, and V. Vogel. 1995. Ordered domains in films of pulmonary surfactant. *Bio-phys. J.* 68:214a. (Abstr.).
- Helm, C., and H. Möhwald. 1988. Equilibrium and nonequilibrium features determining superlattices in phospholipid monolayers. *J. Phys. Chem.* 92:1262–1266.
- Hillenkamp, F., M. Karas, R. C. Beavis, and B. T. Chait. 1991. Matrix-assisted laser desorption/ionization mass spectrometry of biopolymers. *Anal. Chem.* 63:1193–1203.
- Hook, G. E. R., J. W. Spalding, M. J. Ortner, E. G. Tombropoulos, and C. F. Chignell. 1984. Investigation of phospholipid of the pulmonary extracellular lung lining by electron paramagnetic resonance. The effects of phosphatidylglycerol and unsaturated phosphatidylcholines on the fluidity of dipalmitoylphosphatidylcholine. *Biochem. J.* 223:533–542.
- Hwang, J., L. K. Tamm, C. Böhm, T. S. Ramalingam, E. Betzig, and M. Edidin. 1995. Nanoscale complexity of phospholipid monolayers investigated by near-field scanning optical microscopy. *Science*. 270: 610–614.
- Keough, K. M. W. 1992. Physical chemistry of pulmonary surfactant in the terminal air spaces. In *Pulmonary Surfactant: From Molecular Biology to Clinical Practice*. B. Robertson, L. M. G. VanGolde, and J. J. Battenburg, editors. Elsevier, Amsterdam. 109–164.
- Keough, K. M. W., E. Farrel, M. Cox, G. Harrel, and H. W. Tausch, Jr. 1985. Physical, chemical and physiological characteristics of isolates of pulmonary surfactant from adult rabbits. *Can. J. Physiol. Pharmacol.* 63:1043–1051.
- Keough, K. M. W., and N. Kariel. 1987. Differential scanning calorimetric studies of aqueous dispersions of phosphatidylcholines containing two polyenoic chains. *Biochim. Biophys. Acta.* 902:11–18.
- King, R. J., and J. A. Clements. 1972. Surface active materials from dog lung. III. Thermal analysis. *Am. J. Physiol.* 223:727–733.
- King, R. J., M. C. Phillips, P. M. Horowitz, and S. C. Dang. 1986. Interaction between the 35 kDa apolipoprotein of pulmonary surfactant and saturated phosphatidylcholines. Effect of temperature. *Biochim. Biophys. Acta.* 879:1–13.
- Klopper, K. J., and T. K. Vanderlick. 1996. Isotherms of dipalmitoylphosphatidylcholine (DPPC) monolayers: features revealed and features obscure. *J. Colloid Interface Sci.* 182:220–229.
- Kuroki, Y., and T. Akino. 1991. Pulmonary surfactant protein A (SP-A) specifically binds dipalmitoylphosphatidylcholine. *J. Biol. Chem.* 266: 3068–3073.
- Lalchev, Z. I., R. K. Todorov, Y. Tz. Christova, P. J. Wilde, A. R. Mackie, and D. C. Clark. 1996. Molecular mobility in the monolayers of foam films stabilized by porcine lung surfactant. *Biophys. J.* 71:2591–2601.
- Mautone, A. J., K. E. Reilly, and R. Mendelsohn. 1987. Fourier transform infrared and differential scanning calorimetric studies of surface-active material from rabbit lung. *Biochim. Biophys. Acta.* 896:1–10.
- Möhwald, H. 1990. Phospholipid and phospholipid-protein monolayers at the air/water interface. *Annu. Rev. Phys. Chem.* 41:441–476.
- Nag, K., and K. M. W. Keough. 1993. Epifluorescence microscopic studies on monolayers containing mixtures of dioleoyl and dipalmitoylphosphatidylcholine. *Biophys. J.* 65:1019–1026.
- Nag, K., K. M. W. Keough, M. T. Montero, J. Trias, M. Pons, and J. Hernandez-Borrel. 1996c. Evidence of segregation of a quinolone antibiotic in dipalmitoylphosphatidylcholine environment. *J. Lipid Res.* 6:713–736.
- Nag, K., J. Perez-Gil, A. Cruz, and K. M. W. Keough. 1996a. Fluorescently labeled pulmonary surfactant protein C in spread phospholipid monolayers. *Biophys. J.* 71:246–256.
- Nag, K., J. Perez-Gil, A. Cruz, N. H. Rich, and K. M. W. Keough. 1996b. Spontaneous formation of interfacial lipid-protein monolayers during adsorption from vesicles. *Biophys. J.* 71:1356–1363.
- Nag, K., N. H. Rich, C. Boland, and K. M. W. Keough. 1990. Design and construction of an epifluorescence microscopic surface balance for the study of lipid monolayer phase transitions. *Rev. Sci. Instrum.* 61: 3425–3430.
- Nag, K., N. H. Rich, C. Boland, and K. M. W. Keough. 1991. Epifluorescence microscopic observation of monolayers of dipalmitoylphosphatidylcholine: dependence of domain size on compression rates. *Biochim. Biophys. Acta.* 1068:157–160.
- Nag, K., N. H. Rich, and K. M. W. Keough. 1994. Interaction between dipalmitoylphosphatidylglycerol and phosphatidylcholines and calcium. *Thin Solid Films.* 244:841–844.
- Oldfield, E., K. M. Keough, and D. Chapman. 1972. The study of hydrocarbon chain mobility in membrane systems using spin-label probes. *FEBS Lett.* 20:344–346.
- Otis, D. R., Jr., E. P. Ingenito, R. D. Kamm, and M. Johnson. 1994. Dynamic surface tension of surfactant TA: experiments and theory. *J. Appl. Physiol.* 77:2681–2688.
- Perez-Gil, J., K. Nag, S. Taneva, and K. M. W. Keough. 1992. Pulmonary surfactant protein SP-C causes packing rearrangements of dipalmitoylphosphatidylcholine in spread monolayers. *Biophys. J.* 63:197–204.
- Pison, U., R. Herold, and S. Schürch. 1996. The pulmonary surfactant system: biological functions, components, physicochemical properties and alteration during lung disease. *Coll. Surf. A: Physiochem. Engin. Aspects*, 114:165–184.
- Ruano, M. L. F., E. Miguel, J. Pérez-Gil, and C. Casals. 1996. Comparison of lipid aggregation and self-aggregation activities of pulmonary surfactant-associated protein A. *Biochem. J.* 313:683–689.
- Ruano, M. L., K. Nag, L. A. Worthman, C. Casals, J. Perez-Gil, and K. M. Keough. 1998. Differential partitioning of pulmonary surfactant protein SP-A into regions of monolayers of dipalmitoylphosphatidylcholine and dipalmitoylphosphatidylcholine/dipalmitoylphosphatidylglycerol. *Biophys. J.* 74:1101–1109.
- Scarpelli, E. M., and A. T. Mautone. 1994. Surface biophysics of the surface monolayer theory is incompatible with regional lung function. *Biophys. J.* 67:1080–1089.
- Schürch, S., and H. Bachofen. 1995. Biophysical aspects in the design of a therapeutic surfactant. In *Surfactant Therapy for Lung Diseases*. B. Robertson and H. W. Tausch, editors, Marcel Dekker Inc., New York. 3–32.
- Schürch, S., H. Bachofen, J. Goerke, and F. Green. 1992a. Surface properties of rat pulmonary surfactant studied with the captive bubble method: adsorption, hysteresis, and stability. *Biochim. Biophys. Acta.* 1103:127–136.
- Schürch, S., H. Bachofen, and E. R. Weibel. 1985. Alveolar surface tensions in excised rabbit lungs: effect of temperature. *Respir. Physiol.* 62:31–45.
- Schürch, S., J. Goerke, and J. A. Clements. 1976. Direct determination of surface tension in the lungs. *Proc. Natl. Acad. Sci. USA.* 73:4698–4072.
- Schürch, S., F. Possmayer, S. Cheng, and A. M. Cockshutt. 1992b. Pulmonary SP-A enhances adsorption and appears to induce surface sorting of lipid extract surfactant. *Am. J. Physiol.* 263:210–218.
- Schürch, S., D. Schürch, T. Curstedt, and B. Robertson. 1994. Surface activity of lipid extract surfactant in relations to film compression and collapse. *J. Appl. Physiol.* 77:974–986.
- Stine, K. J. 1994. Investigation of monolayers by fluorescence microscopy. *Microsc. Res. Tech.* 27:439–450.
- Träuble, H., H. Eibl, and H. Sawada. 1974. Respiration a critical phenomenon? Liquid phase transition in the lung alveolar surfactant. *Naturwissenschaften.* 61:344–354.



- Teubner, J. K., R. A. Gibson, and E. J. McMurchie. 1983. The influence of water on the phase transition of sheep lung surfactant, a possible mechanism for surfactant phase transition in vivo. *Biochim. Biophys. Acta.* 750:521–525.
- Weis, R. M. 1991. Fluorescence microscopy of phospholipid monolayer phase transitions. *Chem. Phys. Lipids.* 57:227–239.
- Williams, M. C., S. Hawgood, and R. L. Hamilton. 1991. Changes in lipid structure produced by surfactant protein SP-A, SP-B and SP-C. *Am. J. Respir. Cell Mol. Biol.* 5:41–50.
- Yu, S. H., and F. Possmayer. 1993. Adsorption, compression and stability of surface films from natural, lipid extract and reconstituted pulmonary surfactant. *Biochim. Biophys. Acta.* 1167:264–271.